Langmuir

Article

Planar Multilayer Assemblies Containing Block Copolymer Aggregates

Lin Xiao, Renata Vyhnalkova, Miloslav Sailer, Guang Yang, Christopher J Barrett, and Adi Eisenberg

Langmuir, **Just Accepted Manuscript** • Publication Date (Web): 25 Dec 2013

Planar Multilayer Assemblies Containing Block Copolymer Aggregates

‡Lin Xiao,[1,3] ‡Renata Vyhnalkova,[1] Miloslav Sailer,[1] Guang Yang,[3] Christopher J. Barrett,[1,2]

**Adi Eisenberg[1,2]*

[1] Department of Chemistry, McGill University, Otto Maass Building, 801 Sherbrooke St. W, Montreal, Quebec, H3A 2K6, Canada. [2] Centre for Self-Assembled Chemical Structures, McGill University, Otto Maass Building, 801 Sherbrooke St. W, Montreal, Quebec, H3A 2K6, Canada. [3]Department of Biomedical Engineering, College of Life Science and Technology, Huazhong University of Science and Technology, Wuhan 430074, P. R. China. All the research associated with this project was performed at McGill University.

KEYWORDS: Self-Assembly, Block Copolymers, Multilayer Systems, Nanostructures, Layer-by-layer.

ABSTRACT: The design, preparation and properties of planar multilayer structures composed of various combinations of sequentially deposited polyelectrolyte (PE) chains and self-assembled layers of individual block copolymer aggregates (vesicles, micelles or large compound micelles (LCMs)) are described. The aggregates contain negatively or positively charged corona chains while the PE multilayers contain alternating polyanionic or polycationic chains deposited on silicon wafers. The final structures consist of combinations of layers of various charged species: multilayers of alternating PEs of poly(allyl hydrochloride) (PAH) and poly(acrylic acid) (PAA),

as well as vesicles, micelles or large compound micelles of ionized poly(styrene)-b-poly(4-vinyl pyridine) (PS-b-P4VP) or of poly(styrene)-b-poly(acrylic acid) (PS-b-PAA). Two types of layer-by-layer (LbL) multilayer structures were studied: individual aggregate layers sandwiched between PE multilayers, and layers of individual aggregates of various morphologies and of different corona chain charges, deposited on top of each other without intermediate multilayers or individual layers of PEs. The strong interactions between the successive layers are achieved mainly by electrostatic attraction between the oppositely charged layers. The planar LbL multilayers containing block-copolymer aggregates could, potentially, be used as carriers for multiple functional components; each aggregate layer could be loaded with hydrophobic (in the core of the micelles, LCMs or vesicle walls) or hydrophilic functional molecules (in the vesicular cavities). The overall thickness of such planar LbL multilayers can be controlled precisely and can vary from tens of nm to several μm depending on the number of layers, the sizes of the aggregates and the complexity of the structure.

1. Introduction

The LbL self-assembly method of preparing multilayer thin films has proven, over the last twenty years, to be a very useful and versatile technique in surface modification.[1-19] Positively and negatively charged polymers are sequentially adsorbed from dilute solution onto a charged substrate, most commonly by electrostatic interactions, or alternately by hydrogen [5, 13-14] or covalent[6] bonding; this is the basic principle behind the preparation of thin films by the LbL technique.[1-26] The charge overcompensation after the deposition of each layer is the main mechanism by which the buildup of material is achieved.[1-3]

The simplicity, ease and low cost of preparation, coupled with the remarkable nanoscale control of thickness,[9,17] the versatility, environmental friendliness and good biocompatibility of

the LbL assembly technique opens a broad range of applications,[10-23] which vary from biological and therapeutic materials to energy and electrochemical devices. The techniques involved in fabrication of LbL multilayer systems include dip, spray and spin coating, as well as flow based techniques.[1-3,6-7,9,21] The overall range of benefits of the film fabrication method has led to this approach being used in the preparation of LbL systems incorporating, in addition to the simple polyelectrolytes,[7-9] also various other materials, such as small molecule dyes, colloidal particles, enzymes, carbon nanotubes, liposomes and self-assembled aggregates onto planar surfaces.[12-13,16-18,20,22-23]

Independently, self-assembled block copolymer aggregates, such as micelles, rods, vesicles or LCMs, have received considerable attention over past few decades.[27-35] These aggregates usually have a hydrophobic core (micelles, LCMs) or wall (vesicles) and a hydrophilic corona, which makes them stable in aqueous solutions.[27-38] A number of potential applications of self-assembled block copolymer aggregates have been explored. Drug delivery applications [34-35,37-38] are of special interest because of the unique properties of these aggregates. For example, in drug delivery applications, the core of the micelle is capable of incorporating hydrophobic bio-medically active ingredients, which can be delivered to a biological environment because of the stability of the structures by virtue of their hydrophilic coronas. Vesicles can contain hydrophilic species in the hollow centre and possibly also hydrophobic species in the wall in a possible dual delivery system.

Since the hydrophilic corona chains of block copolymer micelles and vesicles can be prepared from PE chains with positive or negative charges and since electrostatic interactions are an inherent aspect of LbL films, it is reasonable to attempt to incorporate charged self-assembled block copolymer aggregates into LbL multilayers. Surprisingly, the literature in this combined

area is scant,[11-16] and only a few of studies have been published dealing with block copolymer aggregates incorporated into PE LbL mulitilayers. For example, Caruso *et al.*[16] prepared self-assembled nanoporous multilayered films using star-like block copolymer micelles of PS-b-PAA and PS-b-P4VP as building blocks. The growth of these nanoporous films is governed by electrostatic and hydrogen-bonding interactions between the opposite block copolymer micelles;[16] these films could potentially be used as reservoirs of various hydrophobic or hydrophilic materials. Zhang et al.[10] fabricated LbL multilayer films by alternating deposition of the poly(styrene-b-poly acrylic acid) (PS-b-PAA) and poly(diallyl-dimethylammonium chloride) loaded with hydrophobic dyes. Hammond et al.[13] studied LbL films composed of self-assembled biodegradable polymeric micelles, which had been loaded with antibacterial material; the antibacterial biodegradable polymeric LbL films were shown to be efficient in bacteria deactivation.[13]

The present paper explores a small part of the enormous range of possibilities of combining polyelectrolyte (PE) multilayers (polyanionic - PAA and polycationic - PAH chains) with charged crew-cut block copolymer aggregates, such as vesicles, micelles and LCMs with anionic or cationic corona chains composed of PS-b-PAA or PS-b-P4VP, deposited on a silicon wafer. Two different structural approaches are utilized, in one of which aggregates are separated by multiple PE layers, while in the other the aggregates of different charge are in direct contact. This publication deals only with structural aspects; filling and release of ingredients will be a subject of a future publication. The morphological and compositional parameter space is extremely large and offers excellent opportunities for optimization, depending on the intended application.

2. Experimental Section

Experimental details are given in the Supporting Information.

3. Results and Discussions

3.1. Aggregate Types

An overview of the individual aggregates used in preparation of the planar LbL multilayer structures, including the preparative conditions, TEM images and sizes of the aggregates, is given in detail in the SI in section 1.5. The aggregates include vesicles of PS-b-PAA (as prepared from various solvents - Type I and Type II), and as well as vesicles, micelles and LCMs of PS-b-P4VP.

3.2. Nomenclature

This study deals with planar LbL structures, composed of layers containing various species, i.e. PE multilayers, vesicles and micelles. In addition, these species carry one of two different charges; therefore the parameter space is large. It is of interest to systematize various structural possibilities of these multilayers by first defining the successive layer possibilities. Figure 1 shows the various possibilities for two layer systems, and is referred to as a structural branch point diagram in this work. A layer which consists of micelles with a positive corona is denoted as M+; similarly a micelle layer with the negative corona are denoted M-. Vesicle layers are labeled as V+ or V-. Polyelectrolyte (PE) multilayers are designated by the letter L and the charge of the top layer, i.e. L+ or L-, depending on whether the charge on the top layer is positive or negative. If necessary, the number of PE layers comprising this multilayer can be denoted by a subscript.

As an example, a layer consisting of negatively charged micelles (M-) can be covered by either a layer of positively charged vesicles (V+) or layer of positively charged micelles (M+) or by a PE multilayer the top layer of which can be either positive or negative (L+ or L-). The six

different possibilities are summarized in the branch point diagram in Figure 1. These are not physical branch points, but branch points on a "tree" of potential multilayer structures, which are schematically shown in the branch point diagram. These branch points can be combined to give "a tree", the components of which are indicated in the diagram below. Two examples of the planar LbL structure, such as $WL_5^+V^-V^+L_6^+$ V^-V^+ and $WL_4^-M^+V^-L_6^-V^+L_5^-V^+M^-$ are given in the SI in Figure 1 and in section 1.6. In section 1.6., the detailed explanation is provided of the order of the layers including the rules involved in preparation of the planar LbL multilayer structures.

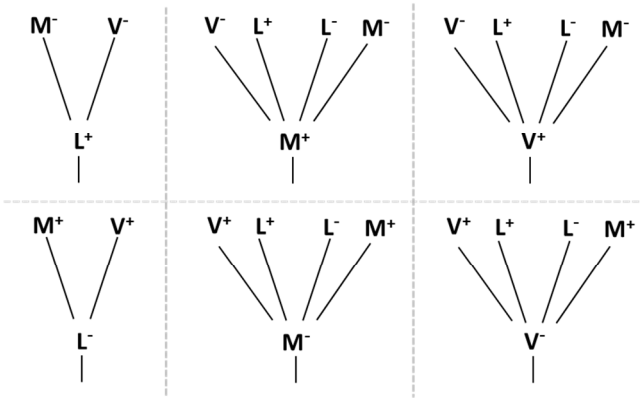

Figure 1. Branch point diagram. M = micelle layer, V = vesicle layer and L = polymer multilayer. The sign on L indicates the charge of the top layer (+ or –). The present branch point diagram utilizes only three species of positive or negative charges.

3.3. LbL Planar Multilayers Composed of Both Polyelectrolytes and Aggregates

The experimental results of structures, prepared in this study, are given below in order of increasing complexity. First, a description of the preparation of the base structure, composed of the PS-b-PAA vesicles deposited on the polyelectrolyte multilayer is discussed. The description of the LbL structure composed of four layers of vesicles of the PS-b-PAA sandwiched between polyelectrolyte multilayers is given next, followed by the description of the LbL structure containing layers of both types of vesicles, i.e. positive (from PS-b-P4VP) and negative (from

PS-b-PAA), deposited between polyelectrolyte multilayers. Two different LbL structures representing different morphologies, i.e. micelles and large compound micelles (LCMs) of PS-b-P4VP, in addition to the PS-b-PAA vesicles deposited between polyelectrolyte multilayers, are described in the SI in sections 1.8. and 1.9. The final structure contains alternating PS-b-PAA (negatively charged) and PS-b-P4VP (positively charged) vesicle layers deposited directly on each other without intermediate polyelectrolyte multilayers. The only PE multilayer in this structure lies between the silicon wafer and the first vesicles layer.

3.3.1. LbL Planar Structure Composed of Polyelectrolyte Multilayers (WL11+).

The first element of the LbL multilayer structure deposited on the silicon wafer is always the PE multilayer. The structure containing only the PE multilayer (shown schematically in Figure 2 in the SI) is the simplest planar LbL structure, discussed in the present study.

3.3.2. LbL Planar Structure Composed of a Vesicle Layer Deposited on a Polyelectrolyte Multilayer (WL11+V- Base Structure).

Figure 2 shows the base LbL planar structure from which all further planar LbL structures of the present study are derived. The base WL11+V- LbL planar structure is shown schematically in Figure 2 A. In analogy to the previous structure, the present structure is composed of eleven alternating negatively charged poly(acrylic acid) (PAA) and positively charged poly(allyl hydrochloride) (PAH) polymer layers, deposited on a silicon wafer. In addition, negatively charged PS_{190}-b-PAA_{34} vesicles are deposited as the top layer. An AFM image of the top view of the WL11+V- LbL planar structure is shown in Figure 2 B. The size of the vesicles ranges from 100 to 200 nm. Some of the vesicles are collapsed due to pressure differences between the interior and exterior of the vesicles during their preparation.[40] As can be seen from the AFM image of the top vesicle layer, generally the vesicles show a rather high

coverage and are randomly distributed over the surface, which indicates that the charge density across the underlying surface is rather high and that the charge distribution on the underlying surface is relatively uniform after modification with the PAH/PAA multilayer. It should be noted that when the positively charged vesicles of PS-b-P4VP were deposited directly on the unmodified silicon wafer, the vesicle coverage was very low (results not shown).

As shown in Figure 2 B, most vesicles are isolated with relatively few contact pairs. The absence of frequent contacts may be an indication of a presence of slightly repulsive interaction between the vesicles arising from the de-protonation of the acrylic acid in milli-Q water as well as the relatively low concentration of vesicles in solution.

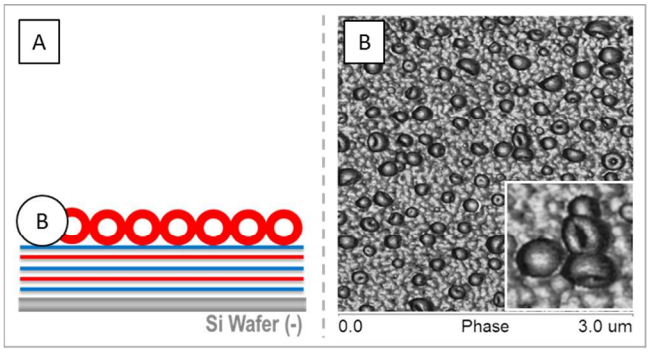

Figure 2. Schematic representation of the side view **A)**, and AFM image of the top view **B)** of $WL_{11}^{+}V^{-}$ LbL planar structure. B) contains an enlarged (2.5 x) view of a small surface segment.

In all figures, the letters in the squares indicate the figure number, while the letters in the circles indicate the layer corresponding to the figure of the same letter, when it is provided. The letter in the square indicates the schematic of the system under discussion.

Table 1 gives an overview of the symbols used in the diagrams describing the multiple layers structures composition.

Symbol							
Morphology	vesicles	vesicles	micelles	LCMs	layer	layer	supporting surface
Polymer	PS-b-PAA	PS-b-P4VP	PS-b-P4VP	PS-b-P4VP	PAA	PAH	Silicon wafer
Charge	-	+	+	+	-	+	-

Table 1. An overview of the symbols used in the composition of multiple layer structures.

3.3.3. LbL Planar Structure Containing Vesicle Layers Deposited Between Polyelectrolyte Multilayers ($WL_{11}^{+}V^{-}$ $L_{17}^{+}V^{-}$ $L_{17}^{+}V^{-}$ $L_{17}^{+}V^{-}$).

3.3.3.1. Surface Topography

Figure 3 represents the $WL_{11}^{+}V^{-}$ $L_{17}^{+}V^{-}$ $L_{17}^{+}V^{-}$ $L_{17}^{+}V^{-}$ planar LbL structure. This system consists of four negatively charged layers of PS-b-PAA vesicles deposited between or on top of PE multilayers. The first (bottom) polyelectrolyte multilayer is composed of 11 alternating layers of PAH or PAA, while each additional polyelectrolyte multilayer consists of 17 alternating layers of PAH/PAA, as represented schematically in Figure 3 A; the sequence $L_{11}^{+}V^{-}$ is deposited first on the silicon wafer, followed by a threefold deposition of the $L_{17}^{+}V^{-}$ sequence. Figures 3 B – E show the AFM images of the top view of each individual vesicle layer. The diameter of the vesicles corresponds to 75 ± 15 nm.

As can be seen from the AFM images, the highest surface density of vesicles is found in the top view AFM images of Figures 3 C and D. The sizes of the vesicles shown in images B and E are smaller than those in C and D. In all cases, it is evident from the AFM images (3 B – D) that the vesicles are randomly distributed over the surface. Compared to the first PS-b-PAA vesicle layer (Figure 3B), the second and third vesicle layers show a somewhat more dense coverage (Figure 3C and 3D). The reason for the slight differences in vesicle surface density in the various layers is not evident.

The differences in the sizes seen in Figures 2 B and 3 B are related to differences in the preparation conditions for the vesicles used; the PS-b-PAA vesicles shown in Figure 2 B were prepared in dioxane while those shown in Figure 3 B were prepared in dioxane/THF mixtures (see sizes in Table 2 in the SI). As can be seen in images 2 B and 3 B, the surface coverage shown in Figure 2 B is higher than that in Figure 2 B. This phenomenon is caused by the difference in numerical vesicle concentration in the solution at the same weight concentration caused by the differences in the size of the vesicles in the two samples. The vesicles shown in the image 3 B were prepared in dioxane, and therefore are larger compared to those prepared in the dioxane/THF mixture; the aggregation number of those prepared from dioxane is 3.1 x 10^{-20} moles of chains/vesicle. The aggregation number of vesicles prepared from dioxane/THF solvent is lower, i.e. 1.1 x 10^{-20} moles of chains/vesicle, therefore the numerical vesicle concentration in the two solutions is different, i.e. 7.3 x 10^{11} and 2.1 x 10^{12} vesicles/mL, respectively. It should be stressed that the polymer concentration in both vesicle solutions is the same, 0.5 mg/mL.

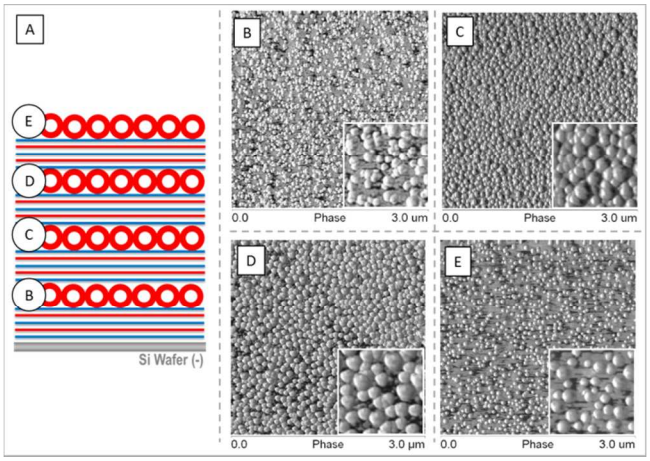

Figure 3. $WL_{11}^{+}V^{-}L_{17}^{+}V^{-}L_{17}^{+}V^{-}L_{17}^{+}V^{-}$ LbL planar structure; A) Schematic representation of the side view of the assembly. B – E) AFM images of the top view of the PS-b-PAA vesicle layers 1 – 4 from bottom. The letters B – E on the schematic representation in A correspond to the AFM images B – E of those layers. B – E contain enlarged (2.5 x) views of small surface segments.

3.3.3.2. Thickness by Ellipsometry

The thickness of the $WL_{11}^{+}V^{-}L_{17}^{+}V^{-}L_{17}^{+}V^{-}L_{17}^{+}V^{-}$ LbL planar structure was studied by ellipsometry at several stages of preparation. The results of the measurements are shown in Figure 4, where the thickness (nm) is plotted as a function of number of individual layers in the structure. As expected, the thickness increases with increasing number of layers, as shown in Figure 4. The thickness of 11 alternating PAH/PAA layers (L_{11}^{+}) corresponds to roughly 50 nm. The addition of the first PS-b-PAA vesicle layer (V^{-}) increases the thickness of the structure by about 35 nm as measured by ellipsometry. This increase in thickness should be related to the average diameter of the vesicles of 75 nm obtained by TEM. However, the average thicknesses, measured by ellipsometry, are expected to be somewhat smaller than the average diameters measured by TEM, which represent a local maximum thickness, not an average. The thickness of the subsequent PAH/PAA multilayer, consisting of 17 alternating layers (L_{17}^{+}) corresponds to roughly 70 nm. The second vesicle layer is ~ 50 nm thick by ellipsometry. According to the results shown in Figure 4, as the additional $L_{17}^{+}V^{-}$ layers are deposited, the thickness of the structure increases by ~ 120 nm; 70 nm of this corresponds to the thickness of 17 alternating PAH/PAA layers and 50 nm to the average thickness contributed by the vesicle layers.

The thickness of the entire $WL_{11}^{+}V^{-}$ $L_{17}^{+}V^{-}$ $L_{17}^{+}V^{-}$ $L_{17}^{+}V^{-}$ LbL planar structure is ~ 460 nm and is, thus below 500 nm (0.5 μm), for this 66 layers structure. In each PE multilayer, the average thickness of a single layer of PAH or PAA is ~4.5 nm.[9] It means the polymer molecules were not deposited as thin layers with flat monolayer chain conformation but as thicker and rougher layers with a loopy conformation.

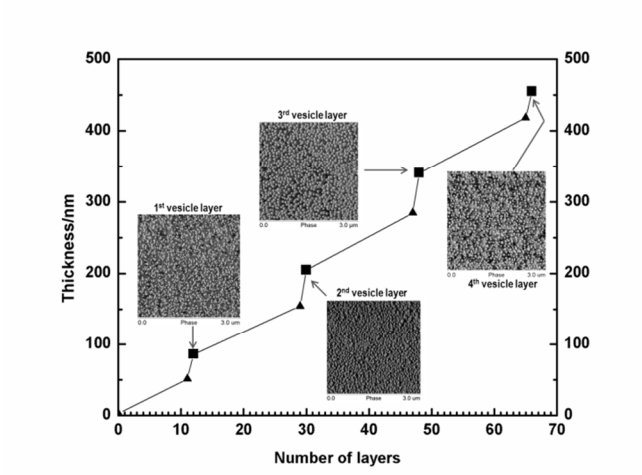

Figure 4. Plot of thickness from ellipsometry *vs.* number of layers in the structure containing four individual layers of PS-b-PAA vesicles between multiple PE layers (schematically shown in Figure 3A). Each large jump in thickness corresponds to a layer of vesicles.

Particle density for the present system, assuming monodisperse vesicles of 75 nm diameter and a distance between vesicle layers of 115 nm, e.g. analogous to the plot in Figure 4, was calculated to be 1.8 x 10^{10} vesicles/cm^2 (square planar packing). Furthermore, with a vertical distance between vesicle layers of 115 nm, the number of layers/cm is 8.7 x 10^4 and the number of vesicles/cm^3 was calculated to be 1.6 x 10^{15} for structures which include the polyelectrolyte multilayers.

3.3.4. LbL Planar Structure Composed of Negatively Charged PS-PAA and of Positively Charged PS-P4VP Vesicle Layers Deposited Between PE Multilayers ($WL_{11}^{+}V^{-}\ L_{10}^{-}V^{+}\ L_{10}^{+}V^{-}$).

The $WL_{11}^{+}V^{-}L_{10}^{-}V^{+}L_{10}^{+}V^{-}$ LbL planar structure, containing both positively and negatively charged vesicles, is shown in Figure 5. The structure consists of 11 PAH/PAA alternating PE layers (L_{11}^{+}) deposited on a silicon wafer, onto the top of which a layer of negatively charged vesicles is deposited. The subsequent multilayer in the present structure consists of 10 alternating layers of PAH/PAA (L_{10}^{-}). The layer of positively charged vesicles (V^{+}) of PS_{473}-b-$P4VP_{36}$ is

introduced next, followed by the deposition of another PE multilayer consisting of 10 alternating layers of PAH/PAA (L_{10}^{+}). The top layer of the structure consists, again, of a layer of negatively charged PS_{188}-b-PAA_{34} vesicles (V^{-}). The average diameter of PS_{188}-b-PAA_{34} vesicles is 110 ± 30 nm, while the average diameter of PS_{473}-b-$P4VP_{36}$ vesicles is 50 ± 18 nm.

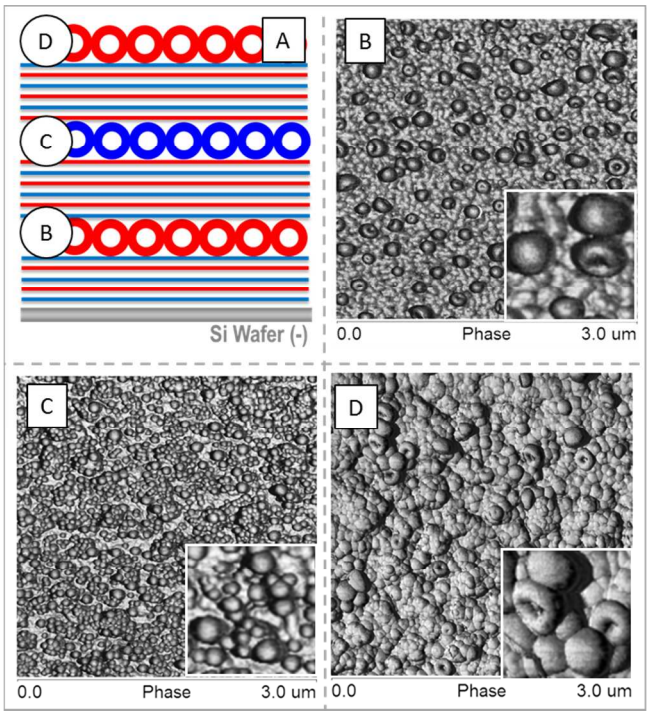

Figure 5. $WL_{11}^{+}V^{-}$ $L_{10}^{-}V^{+}$ $L_{10}^{+}V^{-}$ LbL planar structure; **A)** Schematic representation of the side view of the structure containing PS-b-PAA vesicle layers (B,D) deposited between the PE multilayers and PS-b-P4VP vesicle layer (C). **B) D)** AFM image of the top view of the PS-b-PAA vesicle layer, **C)** AFM image of the surface top view of PS-b-P4VP vesicle layer, B – D contain enlarged (2.5 x) small surface segments.

The total number of layers employed in the present structure is 34, which includes three PE multilayers, two layers of negatively charged vesicles and one layer of positively charged vesicles, as shown in the schematic representation of the side view of the structure in Figure 5 A. AFM images of the top views of the PS-b-PAA vesicle layers (Figure 5 B, D) confirm the

random distribution of the vesicles on the surface; the AFM image of the top view of the PS-b-P4VP vesicle layer (Figure 5 C) confirms a random distribution of the vesicles on the surface as well; however, it can also be seen from the image that the vesicles are smaller than those of the PS-b-PAA vesicles seen in Figures 5 A and 5 C.

It should be noted that the number of layers used to prepare the present LbL planar structure (L_{10}) differs from that in the previously discussed structure (L_{17}). In the previous system, discussed in section 3.3.3, a 17-fold PE multilayer (L_{17}) was employed to sandwich between vesicle layers with the purpose of eliminating completely the topography of the vesicle layer.[39] Moreover, in the previous case, small size PS-b-PAA vesicles (type II, 75$\pm$15 nm) (see table 2 in the SI, section 1.5.) were used to build the vesicle layers with the maximum vesicle coverage. In the present system, however, it was shown that a 10-fold PE multilayer (L_{10}) is sufficient to eliminate the surface influence while providing effective charge density and adhesion[39] for a PS-b-P4VP vesicle layer with a high surface coverage, as shown in Figure 5 C. The higher charge density of the P4VP corona because of the stronger interaction with the top layer of the multilayer film (higher degree of ionization) may explain the high coverage. The differences between the surface coverage shown in images 5 B - D are most likely caused by differences in the vesicle concentration.

As can be seen from Figure 5 D, the top PS-b-PAA vesicle layer in the present structure (Panel 5) shows a lower vesicle coverage compared to the third vesicle layer (3 D Panel 3). The concentration effect is probably the main reason for the surface coverage differences. In addition, it is highly likely that the 10-fold PE multilayer provides less adhesion and a lower charge density compared with the 17-fold PE multilayer.

3.3.5. LbL Planar Structure Composed of Negatively Charged PS-PAA Vesicle and of Positively Charged Micelle Layers Deposited Between PE Multilayers ($WL_{11}^{+}V^{-}L_{10}^{-}M^{+}L_{10}^{+}V^{-}$).

Due to space limitations in the main text of the present publication, the $WL_{11}^{+}V^{-}L_{10}^{-}M^{+}L_{10}^{+}V^{-}$ LbL planar structure, containing micelles in the assembly, is shown schematically in Figure 3 in section 1.8. of the SI.

3.3.6. LbL Planar Structure Composed of a Negatively Charged PS-PAA Vesicle Layers and of Positively Charged Large Compound Micelle (LCM) Layer Deposited Between PE Multilayers ($WL_{11}^{+}V^{-}L_{10}^{-}M^{+}L_{10}^{+}V^{-}$).

The $WL_{11}^{+}V^{-}L_{10}^{-}M^{+}L_{10}^{+}V^{-}$ LbL planar structure described in section 1.8. of the SI is very similar to the $WL_{11}^{+}V^{-}L_{10}^{-}M^{+}L_{10}^{+}V^{-}$ LbL planar structure, discussed in the present section, except that instead of simple micelles described in section 1.8., it contains large compound micelles (LCMs) of PS_{473}-b-$P4VP_{26}$ block-copolymer (M^{+}). The results for the LbL structure containing LCMs are discussed in the Supporting information in section 1.9 in Figure 4.

3.4. LbL Multilayers Composed of Aggregate Layers without an Intermediate PE Layer.

3.4.1. LbL Planar Structure Composed of Alternating Negatively Charged PS-PAA Vesicles and of Positively Charged PS-b-P4VP Vesicles Deposited on Top of Each Other Without Intermediate PE Multilayers ($WL_{11}^{+}V^{-}V^{+}V^{-}V^{+}V^{-}$).

3.4.1.1. Surface Topography

The $WL_{11}^{+}V^{-}V^{+}V^{-}V^{+}V^{-}$ LbL planar structure, containing alternating layers of vesicles of positive and negative charge without employing intermediate PE multilayers between the vesicle layers, is shown schematically in Figure 6 A. The structure, deposited on a silicon wafer, consists of 11 alternating PAH/PAA PE layers (L_{11}^{+}), three layers of negatively charged PS_{188}-b-PAA_{34} vesicles (V^{-}) (B, D and F) and two layers of positively charged vesicles of PS_{473}-b-$P4VP_{36}$ (V^{+})

(C and E). The diameters of PS_{190}-b-PAA_{34} vesicles are ~ 110 ± 30 nm; the averages for the PS_{473}-b-$P4VP_{36}$ vesicles are ~ 50 ± 18 nm. The total number of layers in this structure is 16.

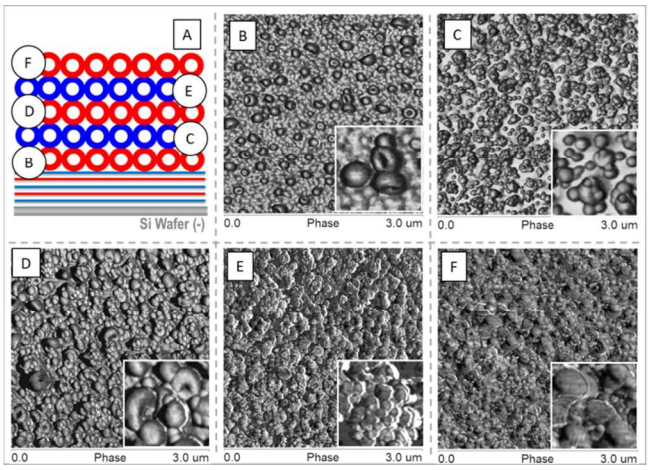

Figure 6. A) Schematic representation of the side view of the structure containing PS-b-P4VP vesicle layers (**C, E**) deposited between PS-b-PAA vesicle layers (**B, D, F**) which are deposited on the PE multiple layer. AFM images of the top view of the **B, D, F)** PS-b-PAA vesicle layer, **C, E)** PS-b-P4VP vesicle layer. **B – F** contain enlargements (2.5 x) of small surface segments.

Figures 6 B, D and F show the AFM images of the top views of the PS-b-PAA vesicle layer surfaces in the structure. An analysis of the images shows that the vesicle sizes correspond to those obtained by TEM (~ 110 nm). It can be seen from the images that the aggregates are randomly distributed on the surfaces. Figures 6 C and 6 E show the AFM images of the top view of the PS-b-P4VP vesicle surfaces. These vesicles are, again, randomly distributed on the surface, but their average diameters are smaller than those of the PS-b-PAA vesicles shown in images 6 B, D and F.

To build the structure shown schematically in Figure 6 A, the vesicle layers were deposited directly on top of each other without any intermediate PE multilayers; as before, adjacent layers are held together by electrostatic interactions between oppositely charged vesicle coronas. From

Figure 6 C, one can see that the small (positively charged) PS-b-P4VP vesicles are mainly attached to the previously adsorbed (negatively charged) somewhat larger PS-b-PAA vesicles, with a relatively lower coverage compared with that shown in Figure 5 C; in that structure, the same PS-b-P4VP vesicles were deposited onto a rough and adhesive PE multilayer. As can be seen in Figure 6 C, there are a few small positively charged PS-b-P4VP vesicles sitting on the surface of the PE multilayer which contains a positively charged PAH as the top layer.

This unusual phenomenon (positively charged vesicles on a positive surface) indicates that in the PE multilayer, there are some negatively charged PAA molecules penetrating into the outermost PAH (positively charged) layer, which makes the PE multilayer surface non uniform and partially negatively charged in some areas. This possible penetration can also explain, in part, the fact that the PS-b-PAA vesicle layers on top of a PE multilayer in all these LBL structures do not show very high vesicle coverage.

Compared with the vesicle layers located between PE multilayers in the LBL structures shown schematically in Panels 3, 5, 3 SI and 4 SI of Figure 8, the vesicle layers in the present structure (Panel 6) in general show a lower surface coverage. This lower coverage can be attributed to the lower contact area between oppositely charged vesicles (in the absence of PE multilayer), which are relatively rigid spheres in direct contact with each other in neighboring layers as compared to top contact area of spheres deposited on a soft flat PE multilayer.

It should be noted that pictures such as those given in Figure 3, Figure 5 and Figure 6 suggest that, in most cases, the small scale topography does not change with number of layers, the only exception being Figure 5D, which shows a slight increase in surface roughness with increasing number of layers. The reason for this uncharacteristic behavior in this particular case is not clear.

As can be seen from AFM images in Figure 2 B, Figure 3, Figure 5 and Figure 6 in the inserts with more highly enlarged sections, the vesicles stay intact upon adsorption since there is no evidence of vesicle brake-up seen on these pictures. The indentations that are seen on some of the vesicles are characteristic of vesicles prepared by the methods we utilize and have been seen in most of vesicles we have prepared right from the beginning of the group investigations of vesicles.[31] It should be recalled that the vesicles are deposited from water at room temperature and that the glass transition temperature of the vesicle wall material, i.e. polystyrene, is ca. 100 ^{O}C, i.e. 75 – 80 ^{O}C above the multilayer preparation temperature. Therefore, no morphological changes are anticipated, or have been observed.

3.4.1.2. Thickness by Ellipsometry

The thickness of the $WL_{11}^{+}V^{-}V^{+}V^{-}V^{+}V^{-}$ LbL planar structure was studied by ellipsometry. The results of the measurements are shown in Figure 7, where the thickness (nm) is plotted as a function of number of individual layers in the structure. As expected, the thickness increases with increasing number of layers. 11 alternating PAH/PAA layers (L_{11}^{+}) correspond to a thickness of roughly 50 nm, which is similar to thickness of 11 alternating PAH/PAA PE layers in case of the $WL_{11}^{+}V^{-}$ $L_{17}^{+}V^{-}$ $L_{17}^{+}V^{-}$ $L_{17}^{+}V^{-}$ planar LbL structure discussed in section 3.3.3.2. The addition of the first PS-b-PAA vesicle layer (V^{-}) increases the thickness of the structure by about 60 nm as measured by ellipsometry. This increase in thickness is much smaller than the average diameter of the vesicles of 110 ± 20 nm obtained by TEM (the data for type I PS-b-PAA vesicles are given in Table 2 in the Supporting Information). The average thicknesses, measured by ellipsometry, are expected to be smaller than the diameter measured by TEM, which represents a local maximum thickness, not an average. The thickness of the subsequent PS-b-

P4VP vesicle layer is roughly 30 nm as measured by ellipsometry. By comparison, the size of the vesicles from TEM is 50 ± 18 nm.

When the third layer of PS-b-PAA vesicles is deposited, the thickness of the structure increases by ~ 60 nm; followed by an increase in thickness ~ 50 nm after the addition of the fourth vesicles layer containing PS-b-P4VP vesicles. The fifth vesicle layer of PS-b-PAA adds an additional 100 nm and the sixth layer, composed of PS-b-P4VP vesicles, adds ca. 50 nm. The total thickness of the $WL_{11}{}^{+}V^{-}V^{+}V^{-}V^{+}V^{-}$ LbL planar structure corresponds to ~ 400 nm, for this 17 layer structure, of which the top six layers are composed of alternating layers of positively and negatively charged vesicles. It should be mentioned that the thickness of each layer, as determined by ellipsometry at different stages of the deposition of the individual layers, and the numerical values of the thicknesses of the individual layers suggest that the structure is non-porous and contains well defined individual layers.

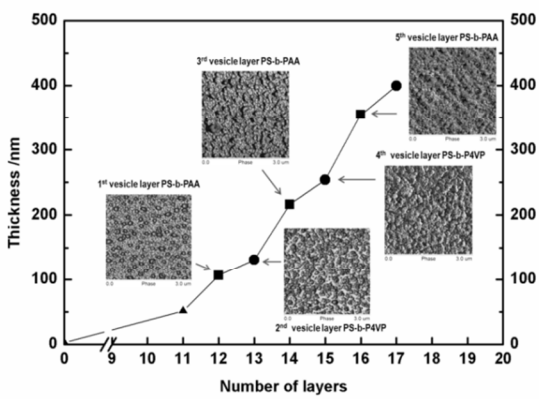

Figure 7. Plot of thickness *vs.* number of layers in the structure containing six alternating individual layers of PS-b-PAA vesicles and PS-b-P4VP vesicles deposited on PE multilayers (schematically shown in Figure 6A); thickness was obtained by ellipsometry.

The thickness curve measured by ellipsometry shows a very similar increase in thickness for each kind of vesicle layer, i.e. PS-b-PAA vesicles or PS-b-P4VP vesicles (on average 90 nm for

PS-b-PAA vesicles and 40 nm for PS-b-P4VP). However, there is a significant difference between the thickness of the first PS-b-PAA vesicle layer and the second PS-b-PAA vesicle layer. The difference suggests that the underlying surfaces of PE multilayer and PS-b-P4VP vesicle layer have different properties. These differences could be possibly related to the different surface topology (spherical structures vs. PE multilayer) or the nature of the PE (PAH vs. P4VP) or both. The final thicknesses of one layer of PS-b-PAA vesicles and one layer of PS-b-P4VP vesicles indicate that rather high vesicle coverage are achieved after several layers of deposition, although full coverage is not achieved, which may be a result of the limited contact area between the relatively rigid vesicles.

It is noteworthy that, as can be seen by comparing Figure 3 and Figure 6, the surface roughness increases with increasing number of vesicle layers in the absence of intermediate PE layers. By contrast, in the presence of intermediate PE layers, the surface roughness does not appear to change with an increase in number of vesicle layers. Earlier studies by Lvov *et al.*[41] on multilayers of virus particles also showed that the roughness can be decreased in the presence of PE layers between the virus layers.

It should be noted that we have no way of calculating precisely the particle density for structures in the absence of PE multilayers because of the necessity for electro-neutrality and the uncertainties in the charge densities of the two types of vesicle under the deposition conditions. It seems reasonable to suggest that the number density should be somewhere between that of PS-PAA vesicles of diameter 110 nm (ca. 8 x 10^{14} vesicles/cm^3 assuming cubic lattice) and that of PS-b-P4VP vesicles of diameter 50 nm (ca. 8 x 10^{15} vesicles/cm^3 assuming cubic lattice, schematically shown in Figure 6 A). Therefore, for the range of systems studied here, the particle density, according to these estimates, is roughly in the same range for structures containing PE

layers (1.6 x 10^{15} Figure 3) as for those without PE multilayers (Figure 6) and, as expected, is clearly related to the diameter of the vesicles, as was shown above.

3.5. Overview of the Planar LbL Multilayer Structures Prepared in the Present Study

An overview of all the structures prepared in the present study is shown schematically in Figure 8. That figure not only describes the detailed structures of the different planar LbL multilayers, but also illustrates the structural relationship between them. To prepare the more complex LbL multilayer structures, one starts with the base structure, shown schematically in Panel 2 in Figure 8. The base consists of a PS-b-PAA vesicle layer deposited on the PAH/PAA alternating PE multilayer, which is placed directly on the silicon wafer. The same structure is used in the preparation of the more complicated LbL multilayers, which are labeled as panels 3, and continuing clockwise to panel 5, 3 SI. 4 SI and 6 in Figure 8. "SI" means the Figure can be found under the same number in the Supporting Information.

The simplest of the complex structures is shown schematically in panel 3 of Figure 8. This structure consists of four PE multilayers alternating with PS-b-PAA vesicle layers. The structure, shown in panel 5 of Figure 8 contains layers of negatively charged PS-b-PAA and positively charged PS-b-P4VP vesicles, alternating with PE multilayers. The structure, labeled as panel 3 SI in Figure 8 contains PE multilayers alternating with two layers of negatively charged PS-b-PAA vesicles and a layer of positively charged PS-b-P4VP micelles. The structure, shown schematically as panel 4 SI in Figure 8, is very similar to the structure in panel 3 SI, except that the simple micelles are replaced by LCMs. The final structure is shown in panel 6 in Figure 8. The structure consists of negatively charged PS-b-PAA vesicle layers alternating with positively charged PS-b-P4VP vesicle layers. The structure is deposited on a PE multilayer on a silicon wafer without intermediate PE multilayers between the vesicle layers.

It is evident that for the planar LbL multilayer structures the parameter space is very large and many combinations of PE multilayers, positively and negatively charged vesicles, micelles, LCMs, LCVs, and even the inclusion of other morphologies in the LbL structures, is likely possible. The present study illustrates some of the simpler examples of complex multilayers that can be achieved using PEs in combination with charged self-assembled block copolymer aggregates.

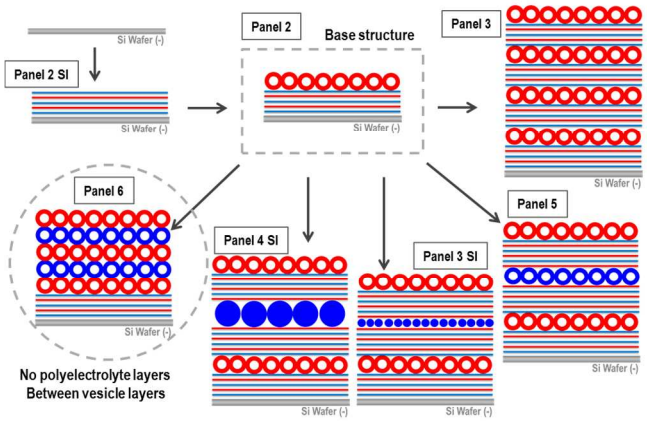

Figure 8. Summary schematic representation of all the structures prepared in the present work. No intermediate PE multilayers were deposited between the individual aggregate layers in case of structure highlighted in the circle. Symbol explanations are given in the Table 1. "SI" in the Panel description means that the images can be found in the Supporting Information, while Panel number without SI means the Figure is given in the main text.

4. Conclusions

This project was devoted to a study of a small part of the wide range of possibilities which arises when one combines sequentially deposited charged PE multilayers and charged aggregates (vesicles, micelles or LCMs). The planar LbL structures are composed of combinations of sequentially deposited layers of various species, such as those self-assembled from PS-b-PAA or

PS-b-P4VP block copolymers aggregates along with alternating poly(anionic) PAA and poly(cationic) PAH PE chains, all deposited on silicon wafers.

Two types of planar LbL multilayer structures were studied: Individual aggregate layers deposited between PE layers, and individual aggregate layers deposited on top of each other without intermediate PE multilayers. The attractive interactions between the successive layers are electrostatic because they occur between oppositely charged chains in the coronas of the aggregates or of PE chains.

This study demonstrates that it is possible to prepare uniform and non-porous multilayer structures containing various combinations of PE multilayers along with distinct layers of charged self-assembled block-copolymer aggregates. It is useful to employ crew-cut block copolymer aggregates to maximize the mobility of aggregates during the deposition and thus assure reasonable layer uniformity. Clearly, given the number of species involved (negatively and positively charged PEs, negatively or positively charged vesicles, micelles or LCMs) the number of possible sequences is very large. Only a small range of the large parameter space was explored in this study and only from a structural point of view.

In exploring the structure and properties of ionisable multilayers containing ionisable self-assembled block copolymer aggregates such as micelles, vesicles or LCMs, it is worth recalling that the aggregates can be very stable or can be made intentionally unstable by the incorporation of appropriate chemical features. As is shown in the study, the coverage of the aggregates in the individual layer can be controlled, among others, by the concentration of aggregates in solution, with a high aggregate concentration leading generally to a high aggregate coverage. Since the aggregates consists of both hydrophobic (walls or cores) and hydrophilic (corona and vesicle cavity) regions, hydrophilic and/or hydrophobic molecules can be incorporated into the

aggregates and thus also into the composite structures. Depending on the specific systems, high loadings may be possible. If multiple ingredients are incorporated into the aggregates, simultaneous release is to be expected. The relative rates of release can be manipulated by the concentration of the ingredients, their interaction parameter with the host, or the nature and location of the species into which they are incorporated.

Finally, this publication describes for the first time the construction of planar LbL structures which contain multiple layers of self-assembled crew cut block copolymer aggregates with or without the use of intervening PE layers yielding non-porous and coherent structures.

ASSOCIATED CONTENT

Supporting Information. The materials used in the preparation of the planar LbL structures are described in detail in section 1.1.; the preparation procedures for the individual aggregates such as vesicles, micelles and large compound micelles (LCMs), are given in section 1.2; the procedures used to prepare the PE multilayers, as well as the deposition of aggregates onto the PE multilayers in alternating fashion, or the deposition of aggregates directly onto other layers of aggregates are explained in section 1.3; the descriptions of the preparation of planar LbL structures include the assembly of these structures containing PE multilayers and layers of positively or negatively charged aggregates alternating with the PE multilayers or deposited on top of each other; the description of the characterization techniques used to evaluate the planar LbL multilayer structures can be found in section 1.4.This material is available free of charge via the Internet at http://pubs.acs.org.

AUTHOR INFORMATION

Corresponding Author

*Adi Eisenberg, Tel.: 514-398-6934, Fax.: 514-398-3797, e-mail: adi.eisenberg@mcgill.ca.

Author Contributions

The manuscript was written through contributions of all authors. All authors have given approval to the final version of the manuscript. ‡Lin Xiao and Renata Vyhnalkova contributed equally

Funding Sources

Financial support by NSERC is gratefully acknowledged.

ACKNOWLEDGMENT

We would like to thank Dr. Futian Liu for synthesizing PS_{297}-b-$P4VP_{30}$ block copolymer and Dr. Tony Azzam for synthesizing PS_{190}-b-PAA_{34} block copolymers, which were prepared in connection with other projects. We would like to thank Mohini Ramkaran for help with AFM imagining.

ABBREVIATIONS

SI Supporting Information, PE polyelectrolyte, PS-b-PAA poly(styrene)-block-poly(acrylic acid), PS-b-P4VP poly(styrene)-block-poly(4-vinyl pyridine), LCMs large compound micelles, LCVs large compound vesicles, PAH poly(allyl hydrochloride), PAA poly(acrylic acid), LbL layer-by-layer, AFM atomic force microscopy, TEM transmission electron microscopy, THF tetra-hydro-furan.

REFERENCES

(1) Decher, G.; Hong, J. D. Buildup of Ultrathin Multilayer Films by a Self-Assembly Process: II Consecutive Adsorption of Anionic and Cationic Bipolar Amphiphiles and Polyelectrolytes on Charged Surfaces. *Ber. Bunsenges. Phys. Chem.*, **1991**, 95, 1430-1434.

(2) Decher, G.; Hong, J. D.; Schmitt, J. Buildup of Ultrathin Multilayer Films by a Self-assembly Process: III. Consecutively Alternating Adsorption of Anionic and Cationic Polyelectrolytes on Charged Surfaces. *Thin Solid Films*, **1992**, 210/211, 831.

(3) Decher, G. Fuzzy Nanoassemblies: Toward Layered Polymeric Multicomposites. *Science*, **1997**, 277, 1232-1237.

(4) Quinn, J.F.; Johnston, P.R.A.; Such, G.K.; Zelikin, A.N.; Caruso, F. Next Generation, Sequentially Assembled Ultrathin Films: Beyond Electrostatics. *Chem. Soc. Rev.,* **2007**, 36, 707-718.

(5) Such, G.K.; Johnston, A.P.R.; Caruso, F. Engineered Hydrogen-Bonded Polymer Multilayers: From Assembly to Biomedical Applications. *Chem. Soc. Rev*., **2011**, 40, 19-29.

(6) Gill, R., Mazhar; M., Felix; O., Decher, G. Covalent Layer-by-Layer Assembly and Solvent Memory of Multilayer Films from Homobifunctional Poly(dimethylsiloxane). *Angew. Chem. Int. Ed*., **2010**, 49, 6116-6119.

(7) Burke, S. E.; Barrett, C. J. Swelling Behavior of Hyaluronic Acid/Polyallylamine Hydrochloride Multilayer Films. *Macromolecules*, **2004**, 37, 5375-5384.

(8) Mermut, O.; Lefebre, J.; Gray, D. G.; Barrett, C. J. Structural and Mechanical Properties of Multilayer Films Studied by AFM. *Macromolecules*, **2003**, 36, 8819-8824.

(9) Mendelson, J. D.; Barrett, C. J.; Chan, V. V.; Pal, A. J.; Mayes, A. M.; Rubner, M. F. Fabrication of Microporous Thin Films from Polyelectrolyte Multilayers. *Langmuir,* **2000**, 16, 5017-5021.

(10) Ma, N., Zhang; H., Song, B.; Wang, Z.; Zhang, X. Polymer Micelles as Building Blocks for Layer-by-Layer Assembly: An Approach for Incorporation and Controlled Release of Water-Insoluble Dyes. *Chem. Mater.*, **2005**, 17, 5065-5069.

(11) Zhu, Z.; Sukhishvili, S.A. Layer-by-layer Films of Stimuli-responsive Block Copolymer Micelles. *J. Mater. Chem*., **2012**, 22, 7667-7671.

(12) Kim, T.G.; Lee, H.; Jang, Y.; Park, T.G. Controlled Release of Paclitaxel from Heparinized Metal Stent Fabricated by Layer-by-Layer Assembly of Polylysine and Hyaluronic Acid-*g*-Poly(lactic-*co*-glycolic acid) Micelles Encapsulating Paclitaxel. *Biomacromolecules*, **2009**, 10, 1532-1539.

(13) Kim, B.-S.; Park, S.W.; Hammond, P.T. Hydrogen-Bonding Layer-by-Layer-Assembled Biodegradable Polymeric Micelles as Drug Delivery Vehicles from Surfaces. *ACS Nano*, **2008**, 2, 2, 386-392.

(14) Nguyen, P.M.; Zacharia, N.S.; Verploegen, E.; Hammond, P. Extended Release Antibacterial Layer-by-Layer Films Incorporating Linear-Dendritic Block Copolymer Micelles. *Chem. Mater.,* **2007**, 19, 5524-5530.

(15) Qi, B.; Tong, X.; Zhao, Y. Layer-by-Layer Assembly of Two Different Polymer Micelles with Polycation and Polyanion Coronas. *Macromolecules*, **2006**, 39, 5714-5719.

(16) Cho, J.; Hong, J.; Char, K.; Caruso, F. Nanoporous Block Copolymer Micelle/Micelle Multilayer Films with Dual Optical Properties. *J. Am. Chem. Soc.,* **2006**, 128, 9935-9942.

(17) Michel, M.; Izquierdo, A.; Decher, G.; Voegel, J.- C.; Schaaf, P.; Ball, V. Layer by layer Self-assembled Polyelectrolyte Multilayers with Embedded Phospholipid Vesicles Obtained by Spraying: Integrity of the Vesicles. *Langmuir*, **2005**, 21, 7854-7859.

(18) Michel, M.; Vautier, D.; Voegel, J.- C.; Schaaf, P.; Ball, V. Layer by layer Self-assembled Polyelectrolyte Multilayers with Embedded Phospholipid Vesicles. *Langmuir*, **2004**, 20, 4835-4839.

(19) Lee, J.-S.; Cho, J.; Lee, Ch.; Kim, I.; Park, J.; Kim, Y.-M.; Shin, H.; Lee, J.; Caruso, F. Layer-by-layer Assembled Charge-trap Memory Devices with Adjustable Electronic Properties. *Nature Nanotech.*, **2007**, 2, 790-795.

(20) Caruso, F.; Caruso, R. A.; M□hwald, H. Nanoengineering of Inorganic and Hybrid Hollow Spheres by Colloidal Templating. *Science*, **1998**, 282, 1111-1114.

(21) Schneider, G.F.; Decher, G.; Nerambourg N.; Praho R.; Werts M.H.; Blanchard-Desce M. Distance-dependent Fluorescence Quenching on Gold Nanoparticles Ensheathed with Layer-by-layer Assembled Polyelectrolytes. *Nano Lett.*, **2006**, 6, 3, 530-536.

(22) Tedeschi, C.; Caruso, F.; Mohwald, H.; Kirstein, S. Adsorption and Desorption Behavior of an Anionic Pyrene Chromophore in Sequentially Deposited Polyelectrolyte-Dye Thin Films. *J. Am. Chem. Soc.*, **2000**, 122, 5841-5848.

(23) Lvov, Y.; Caruso, F. Biocolloids with Ordered Urease Multilayer Shells as Enzymatic Reactors. *Anal. Chem.*, **2001**, 73, 4212-4217.

(24) Yoo, D.; Shiratori, S.S.; Rubner, M.F. Controlling Bilayer Composition and Surface Wettability of Sequentially Adsorbed Multilayers of Weak Polyelectrolytes. *Macromolecules*, **1998**, 31, 4309-4318.

(25) Cho, J.; Caruso, F. Polymeric Multilayer Films Comprising Deconstructible Hydrogen-Bonded Stacks Confined between Electrostatically Assembled Layers. *Macromolecules*, **2003**, 36, 2845-2851.

(26) Dubas, S.T.; Schlenoff, J.B. Factors Controlling the Growth of Polyelectrolyte Multilayers. *Macromolecules*, **1999**, 32, 8153-8160.

(27) Kwon, A. V.; Kataoka, K. Block copolymer micelles as long-circulating drug vehicles, *Adv. Drug Deliver. Rev.,* **1995**, 16, 295-309.

(28) Kabanov, A.V.; Alakhov, V. Y.; Alexandris, P.; Lindman, B. *Amphiphilic Block Copolymers: Self Assembly and Applications,* Eds.: Elsevier: Amsterdam, **1997**.

(29) Torchilin, V.P. Micellar Nanocarriers: Pharmaceutical Perspectives. *Pharm. Res.*, **2007**, 24 1, 1-16.

(30) Gindy, M.E.; Panagiotopoulos, A.Z.; Prud'homme, R.K. Composite Block Copolymer Stabilized Nanoparticles: Simultaneous Encapsulation of Organic Actives and Inorganic Nanostructures. *Langmuir*, **2008**, 24, 83-90.

(31) Zhang, L.F.; Eisenberg, A. Multiple Morphologies of "Crew-Cut" Aggregates of Polystyrene-*b*-poly(acrylic acid) Block Copolymers. *Science*, **1995**, 268, 1728-1731.

(32) Wilhelm, M.;, Zhao, Ch.-L.;, Wang, Y.; Xu, R.; Winnik, M. A.; Mura, J.-L.; Riess, G.; Croucher, M.D. Poly(styrene-ethylene oxide) Block Copolymer Micelle Formation in Water: a Fluorescence Probe Study. *Macromolecules*, **1991**, 24, 1033-1040.

(33) Giacomelli, C.; Schmidt, V.; Borsali, R. Specific Interactions Improve the Loading Capacity of Block Copolymer Micelles in Aqueous Media. *Langmuir*, **2007**, 23, 6947-6955.

(34) Vyhnalkova, R; Eisenberg, A.; van de Ven, T. Ten Million Fold Reduction of Live Bacteria by Bactericidal Filter Paper. *Adv. Funct. Mater.,* **2012**, 22, 19, 4096-4100.

(35) Vyhnalkova, R.; Eisenberg, A.; van de Ven, T. Loading and Release Mechanisms of a Biocide in Polystyrene-block-poly(acrylic acid) Block Copolymer Micelles. *J. Phys. Chem.*, **2008**, 112, 8477-8485.

(36) Jain, S.; Bates, F. S. On the Origins of Morphological Complexity in Block Copolymer Surfactants. *Science,* **2003**, 300, 460-464.

(37) Mai, Y.; Eisenberg, A. Controlled Incorporation of Particles into the Central Portion of Block Copolymer Rods and Micelles. *Macromolecules*, **2011**, 44, 3179-3184.

(38) Mai, Y.; Xiao, L.: Eisenberg, A. Morphological Control in Aggregates of Amphiphilic Cylindrical Metal–Polymer "Brushes". *Macromolecules*, **2013**, 46, 3183-3189.

(39) Sailer, M.; Barrett, C. J. Fabrication of Two-Dimensional Gradient Layer-by-Layer Films for Combinatorial Biosurface Studies. *Macromolecules,* **2012**, 45, 5704-5711.

(40) Azzam, T.; Eisenberg, A. Fully Collapsed (Kippah) Vesicles: Preparation and Characterization. *Langmuir*, **2010**, 26, 10513- 10523.

(41) Lvov, Y.; Haas, H.; Decher, G.; M□hwald, H.; Mikhailov, A.; Mtchedlishively, B.; Morbunova, E.; Vainshtein, B. Successive Deposition of Alternate Layers of Polyelectrolytes and Charged Virus. *Langmuir*, **1994**, 10, 4232-4236.

SYNOPSIS TOC: The present publication deals with a layer by layer deposition on flat surfaces of charged polyelectrolyte chains and charged self-assembled block copolymer aggregates, which are used in the preparation of multiple layer structures.

TOC Graphics: